Optical Theorem Helps Understand Thresholds of Lasing in Microcavities with Active Regions

Elena I. Smotrova, *Member, IEEE,* Volodymyr O. Byelobrov, *Student Member, IEEE,* Trevor M. Benson, *Senior Member, IEEE,* Jiří Čtyroký, *Senior Member, IEEE,* Ronan Sauleau, *Senior Member, IEEE,* and Alexander I. Nosich, *Fellow, IEEE*

***Abstract*— Within the framework of the recently proposed approach to view the lasing in open microcavities as a linear eigenproblem for the Maxwell equations with exact boundary and radiation conditions, we study the correspondence between the modal thresholds and field overlap coefficients. Macroscopic gain is introduced into the cavity material within the active region via the "active" imaginary part of the refractive index. Each eigenvalue is constituted of two positive numbers, namely, the lasing wavenumber and the threshold value of material gain. This approach yields clear insight into the lasing thresholds of individual modes. The Optical Theorem, if applied to the lasing-mode field, puts the familiar "gain = loss" condition on firm footing. It rigorously quantifies the role of the spatial overlap of the mode E-field with the active region, whose shape and location are efficient tools of the threshold manipulation. Here, the effective mode volume in open resonator is introduced from first principles. Examples are given for the 1-D cavities equipped with active layers and distributed Bragg reflectors and 2-D cavities with active disks and annular Bragg reflectors.**

***Index Terms*— Eigenvalue problem, lasing threshold, microcavity laser, optical theorem, overlap coefficient.**

Manuscript received November 23, 2009; revised May 3, 2010; accepted June 13, 2010. Date of current version October 15, 2010. This work was supported in part by the National Academy of Sciences of Ukraine (NASU), under Project 09/36-H, in part by the Ministry of Education and Science, Ukraine, under Project M/146-2010, in part by the Royal Society, under Joint Project IJP-2007/R1-FS, in part by the Academy of Sciences of the Czech Republic (ASCR), jointly with NASU, under the Exchange Project, in part by the European Science Foundation under the research network "Newfocus," in part by the International Visegrad Fund through a Ph.D. scholarship to V. O. Byelobrov, and in part by the Brittany Region, France, through a research professorship to A. I. Nosich.

E. I. Smotrova and V. O. Byelobrov are with the Institute of Radiophysics and Electronics, the National Academy of Sciences of Ukraine, Kharkiv 61085, Ukraine (e-mail: elena_smotrova@yahoo.com; volodia.byelobrov@gmail.com).

A. I. Nosich is with the Universite Europeenne de Bretagne, Institute d'Electronique et Telecommunications de Rennes, Universite de Rennes 1, Rennes 35042, France. He is also with the Institute of Radiophysics and Electronics, the National Academy of Sciences of Ukraine, Kharkiv 61085, Ukraine (e-mail: anosich@yahoo.com).

T. M. Benson is with the George Green Institute for Electromagnetics Research, University of Nottingham, Nottingham NG7 2RD, U.K. (e-mail: trevor.benson@nottingham.ac.uk).

J. Čtyroký is with the Institute of Photonics and Electronics, ASCR v.v.i., Prague 8 18251, Czech Republic (e-mail: ctyroky@ufe.cz).

R. Sauleau is with the Institute d'Electronique et Telecommunications de Rennes, Universite de Rennes 1, Rennes 35042, France (e-mail: ronan.sauleau@univ-rennes1.fr).

Color versions of one or more of the figures in this paper are available online at http://ieeexplore.ieee.org.

Digital Object Identifier 10.1109/JQE.2010.2055836

I. Introduction

COMPREHENSIVE microlaser models try to account for several physical mechanisms, most notable of them being transport of carriers, heating, and optical confinement, coupled together in a nonlinear manner [1]–[3]. Still, useful information can be obtained if all non-electromagnetic effects are neglected, and the optical modes are viewed as solutions of the linear set of source-free Maxwell equations.

Until recently, linear modeling of microdisk and other microcavity lasers has implied exclusively the calculation of the natural modes of the "cold" or, equivalently, *passive* open dielectric resonators. Mathematically, this means solving the time-harmonic Maxwell eigenvalue problem for the complex-valued natural frequencies ω or wavenumbers $k = \omega/c$, where c is the free-space light velocity. These eigenvalues form a *discrete* set and hence can be numbered using, say, the index s. Then the modes with the largest Q factors, i.e., $Q_s = \mathrm{Re}k_s/2|\mathrm{Im}k_s|$, are associated with the lasing [4]. The eigenfunctions corresponding to these eigenvalues are the modal fields; they decay in time as $e^{-|\mathrm{Im}k_s|ct}$ but grow in space as $e^{|\mathrm{Im}k_s|R}/R$ far from the cavity ($\vec{R} = \{R, \theta, \varphi\}$).

Analytical treatment of microcavity modes is possible only in the canonical cases of plane-parallel [in (1-D)], concentric circular [in (2-D)] and spherical [in (3-D)] geometries, where the rigorous separation of variables leads to explicit characteristic equations. Still, simple shapes are not always easy for analysis; for instance, even a rough analytical estimation of Q factor of a whispering gallery (WG) mode needs fine techniques based on elaborate asymptotics of special functions [5]. That is why, although formulas for mode frequencies in 2-D cavities with annular Bragg reflectors (ABRs) are found in [6], [7], their Q factors are absent there. Computing the complex eigenfrequencies from the associated determinantal equations is also a painful task because of the mode couplings. Therefore, some authors, like [8], try to avoid it by using the "alternative" definition of Q factor as the ratio between the stored and lost powers. We will discuss this relation later; here, we only note that, if used alone, this expression does not show that the eigenfrequencies are discrete and (erroneously) suggests thinking that Q factor is a continuous function of frequency. To avoid this pitfall, one should always use the mathematical definition as given above.

Note that geometrical optics, in the form of the billiards theory [9]–[11], has led to important discoveries like the

"bow-tie" modes in stadium cavities, but fails to quantify the modal Q factors. Adding the Snell law and Fresnel coefficients has limited effect, as it is based on the assumption of a locally flat boundary illuminated by a plane wave, and realistic microcavities are far from this situation. Besides, billiards theory fails to grasp the mode discreteness.

On the other hand, finite difference time domain (FDTD) codes that are important today are not able to solve the eigenvalue problems directly. Evaluation of the Q factors is done via studying Fourier transform of a transient signal [12]. The result depends on the size and shape of computation window and the choice of the source and observation points, suffers from the staircasing of the cavity boundary, and needs prohibitively large time intervals in the numerical Fourier transform to visualize the peaks with $Q > 10^5$ [13]–[15].

Therefore, a powerful current trend (see [16]) is the use of integral equation (IE) methods [17]–[21]. As a matter of fact, the IE approach proves that viewing dielectric open resonators as stable, unstable, or chaotic is pointless with full-wave formalism; the chaos appears only in ray-like approximation.

In general, cold-cavity modeling has proved to be an adequate way for predicting the frequency of lasing, which is determined by the cavity shape, size, and material. Moreover, tailoring the shape has become a widely recognized engineering tool for improving the emission directionality [11].

The lasing phenomenon, however, is not addressed directly through the Q factor; neither the presence of the active region nor the specific value of material gain that is needed to force a mode to lase is included in the formulation. As a result, the Q-factor theory is unable to explain why in a stadium-shape cavity the lasing often occurs in the "bow-tie" modes, whose Q factors are several orders lower than those of the WG-like modes [22]. To answer this question, complicated nonlinear descriptions of the lasing have been proposed [23], [24]. A similar situation is the effect of the lower threshold photopump power for the WG-mode microdisk laser with a hollow pump beam [25]. The mentioned drawback is quite unfortunate, as most of the microcavity lasers either use spatially nonuniform pumping or contain active regions optically coupled with passive elements such as distributed Bragg reflectors (DBRs).

The idea of introducing material gain to simulate the lasing had been in the air since the invention of lasers. Physically transparent "gain = loss" condition has become a ubiquitous tool in semiclassical laser physics [1], [26], [27] based on the ray-tracing (essentially 1-D) model of a laser cavity. To determine the lasing frequency, another phenomenological condition of the 2π-multiple increment of the phase of optical ray making one roundtrip in such a cavity is also necessary.

On the other hand, in the 1970s there appeared a brief and intensive discussion on the scattering by "negative-absorption" particles [28], [29]. This research, however, was abandoned after it was realized that, in the scattering problem, infinitely large scattered fields could be obtained. Solving the eigenfrequency problem in the presence of gain is free from that defect. It was attempted in [30], and the conditions of obtaining $\mathrm{Im}k_s = 0$ were studied. A similar approach had been used sometimes when studying vertical cavity surface-emitting lasers (VCSELs) and other lasers [31]–[36]. More recently, active ABR resonators were studied in 2-D [37] and quasi-3-D manner [38], [39] using eigenvalue problems.

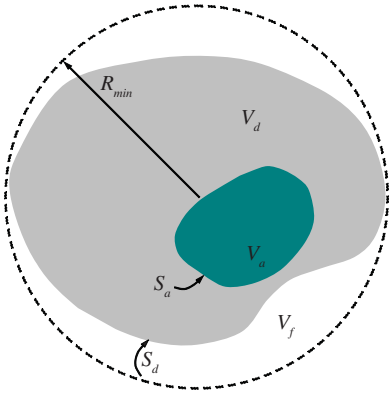

Fig. 1. Generic geometry of a microcavity with a partial active region.

Unlike the latter publications and the earlier ones, [40] presented a complete Maxwellian formulation of the lasing eigenvalue problem (LEP) and systematically applied it to the active circular cavity as a 2-D model of uniformly active thin microdisk. Further studies of stand-alone and coupled microlasers within this formulation can be found in [41]–[47].

In the remainder of this paper, Section II gives the problem formulation and presents the Optical Theorem (OT). General properties of the fully and partially active cavities are considered in Sections III and IV, respectively. Sections V and VI, respectively, present illustrative numerical data for the lasing modes in flat-layered (1-D) and circular-concentric (2-D) cavities. Conclusions are summarized in Section VII.

II. Optical Theorem for Lasers

A. Basic Equations

Consider a generic 3-D laser geometry shown in Fig. 1. Here V_d and V_a are passive-dielectric and active-dielectric regions with boundaries S_d and S_a, respectively, and $V_{\min}$ is the domain inside the so-called minimum sphere, i.e., a sphere of the minimum radius $R_{\min}$ containing both V_d and V_a. Note that it may or may not contain a free space part V_f, and hence the whole passive part of the open cavity is $V_p = V_d + V_f$. The importance of the minimum sphere is that, outside of it, the field is a superposition of solely outgoing waves while inside the field contains the ingoing waves as well: this is what is necessary to build a resonance.

In LEP, we seek real-valued pairs of numbers (k, γ), which generate nonzero time-harmonic fields $\{\vec{E}, \vec{H}\}e^{-i\omega t}$, by solving off, S_d and S_a, the set of Maxwell equations

$$\mathrm{curl}\ \vec{E} = ikZ_0\vec{H}, \quad \mathrm{curl}\ \vec{H} = -ik\nu^2 Z_0^{-1}\vec{E} \tag{1}$$

where $Z_0 = (\mu_0/\varepsilon_0)^{1/2}$ is free-space impedance, $k = \omega/c$, the piecewise-constant refractive index ν equals 1 in V_f and out of $V_{\min}$, α_d in V_d ($Im\alpha_d \geq 0$), and $\alpha_a - i\gamma \quad (\alpha_a, \gamma > 0)$ in V_a, and all materials are assumed nonmagnetic. On S_d and S_a, the continuity conditions are requested

$$\vec{E}^-_{\tan} = \vec{E}^+_{\tan}, \quad \vec{H}^-_{\tan} = \vec{H}^+_{\tan} \tag{2}$$

where the superscripts "±" refer, respectively, to the limiting values of the functions from inside and outside S_d or S_a, and

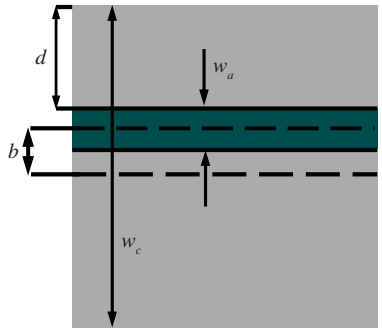

Fig. 2. Quantum well buried in a passive slab cavity in free space.

the subscript "tan" is for the field components lying tangential to them. Besides, the time-averaged electromagnetic energy must be locally integrable to prevent source-like singularities

$$\int_{V\subset R^3}\left[Z_0^{-1}\mathrm{Re}\left(\nu^2\right)|\vec{E}|^2+Z_0|\vec{H}|^2\right]dv<\infty. \tag{3}$$

Further, a *condition at infinity*, at $R\to\infty$, must be added. If the domains V_d and V_a are finite and k is real-valued, this is the Silver–Muller radiation condition [48]

$$\lim_{R\to\infty}\left\{\vec{E}(\vec{R})-Z_0\vec{H}(\vec{R})\times\vec{R}/R\right\}=0. \tag{4}$$

This vector condition provides for the spherical-wave behavior at infinity and, in addition, eliminates non-transverse field components. In 1-D and 2-D problems, it reduces to the scalar Sommerfeld radiation condition. One can equivalently write (4) as a set of asymptotic requests [48]

$$\begin{aligned}E_\varphi=Z_0H_\theta&\sim\frac{e^{ikR}}{kR}\Phi^{(1)}(\theta,\varphi),\ E_R,H_R\sim 0\\ E_\theta=-Z_0H_\varphi&\sim\frac{e^{ikR}}{kR}\Phi^{(2)}(\theta,\varphi),\ R\to\infty\end{aligned} \tag{5}$$

where dimensionless angular-pattern functions $\Phi^{(1,2)}(\theta,\varphi)$ indirectly depend on k, γ, α_d, α_a, and S_d, S_a.

The fundamental properties of the lasing eigenvalues can be established for an arbitrary open cavity with an active region. This is based on the analytical regularization (see [49]), i.e., equivalent reduction of the boundary-value problem (1)–(4) to a set of the Fredholm second-kind boundary IEs of Muller's type [50], and the use of the operator extensions of the Fredholm theorems [51]. It is found that the eigenvalues form a discrete set on the plane (k,γ), so that they can be counted with the aid of some index, say s; each (k_s,γ_s) has finite multiplicity and depends on S_d, S_a and α_d, α_a in a piece-continuous or piece-analytic manner, and this property can be lost only if eigenvalues coalesce.

For the separable geometries, the same conclusions follow simply from the theorems of complex calculus. Note also that the gain per unit length, which is the traditional quantity in the descriptions of the Fabry–Perot cavities, is $g=k\gamma$.

B. Optical Theorem for Passive and Active Cavities

A very instructive insight into the nature of lasing is obtained from the OT applied to the LEP (1)–(4). As is known, in the time-harmonic plane wave scattering, OT links the total extinction cross section of a scatterer with the amplitude of the forward-scattered field in the far zone. Mathematically, this is the result of application of the vector Green's formula to the total field, which satisfies time-harmonic Maxwell equations, and its complex conjugate [52, p. 98]. The most general form of such expression is the Complex Poynting Theorem (CPT). For the complex k, this is

$$\begin{aligned}\Pi=&-(1/2)\int_V\left(\vec{j}^{e*}\vec{E}+\vec{j}^{m}\vec{H}^*\right)dv\\&+(i/2)\int_V\left(k^*\varepsilon^*Z_0^{-1}|\vec{E}|^2-k\mu Z_0|\vec{H}|^2\right)dv\end{aligned} \tag{6}$$

where

$$\Pi=(1/2)\oint_S\vec{E}\times\vec{H}^*ds \tag{7}$$

is the total outward flux of the Poynting vector through the arbitrary boundary S enclosing a volume V containing all scatterers and sources, $\varepsilon=\nu^2$ and μ are the relative permittivity and permeability, respectively, $\vec{j}^e$ and $\vec{j}^m$ are given electric and magnetic currents, respectively (i.e., the sources), and the asterisk means complex conjugation.

CPT (6) can be also applied to a *natural mode* number s (in this case, $\vec{j}^e=\vec{j}^m=0$) in a *passive open cavity* (i.e., with $V_a=0$), having complex eigenfrequency k_s. On the extraction of the real part, we retrieve the remarkable formula

$$-\frac{\mathrm{Re}k_s}{\mathrm{Im}k_s}=\frac{W_s}{W_{abs(s)}+W_{rad(s)}} \tag{8}$$

$$W_s=(1/2)\int_{V_{\min}}\left(Z_0^{-1}\mathrm{Re}\varepsilon|\vec{E}_s|^2+Z_0\mathrm{Re}\mu|\vec{H}_s|^2\right)dv \tag{9}$$

$$W_{abs(s)}=(1/2)\int_{V_{\min}}\left(Z_0^{-1}\mathrm{Im}\varepsilon|\vec{E}_s|^2+Z_0\mathrm{Im}\mu|\vec{H}_s|^2\right)dv \tag{10}$$

$$W_{rad(s)}=\mathrm{Re}\Pi_s/\mathrm{Re}k_s \tag{11}$$

where W_s, $W_{abs(s)}$, and $W_{rad(s)}$ are the powers stored in, absorbed in, and radiated from open cavity, and $\mathrm{Re}\Pi_s$ is the full time-averaged flux of the mode Poynting vector out of the minimum sphere. Either side of (8) is simply $2Q_s$ and hence can be considered as a rigorous definition of the Q factor. It is therefore "rigidly" linked to the mode, i.e., may take only discrete values. Note that a frequent misunderstanding [26, p. 218] is that calculating the open-cavity Q factor via the right-hand part (RHP) of (8) is impossible because of the field divergence at $R\to\infty$. This is so only if W_s is calculated as the power contained in finite volume (e.g., in dielectric) while the power flux $P_{rad(s)}$ is considered at $R\to\infty$: then the latter quantity indeed diverges because of $\mathrm{Im}k_s<0$. Rigorous treatment of the $V_{\min}$ replacement with the whole space in (9) shows that then (8) turns into a trivial identity (both sides are $-\mathrm{Re}k_s/\mathrm{Im}k_s$). Thus, for an open cavity the RHP of (8) is indeed useless if one takes $R\to\infty$, however by a different reason. Now, turn to the LEP and apply (6) to the *lasing mode* field $\{\vec{E}_s,\vec{H}_s\}$ taking into account that sources are absent, $\mathrm{Im}k_s=0$, and $V_a\neq 0$. The result is the *OT for lasers*

$$\tilde{W}_{rad(s)}+\tilde{W}_{abs(s)}=\tilde{W}_{gain(s)} \tag{12}$$

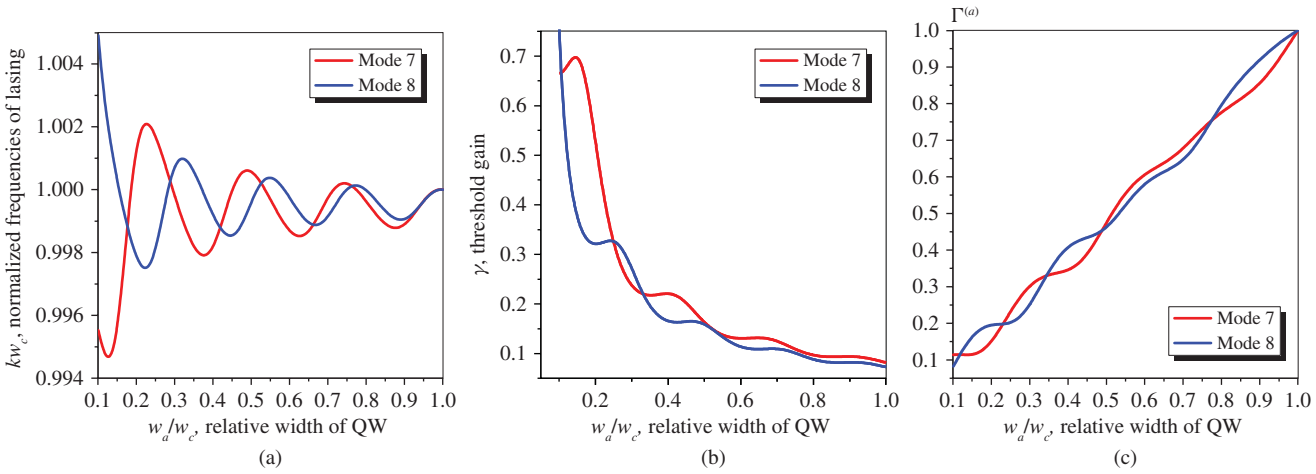

Fig. 3. (a) Normalized lasing frequencies, (b) thresholds, and (c) overlap coefficients of the modes $n = 7$ and 8 in the slab cavity with a centered QW vs. the normalized relative width of the active region. $\alpha_a = \alpha_p = 3.53$. The frequencies are normalized by their limit values at $w_a = w_c$.

$$\tilde{W}_{gain(s)} = Z_0^{-1}\gamma_s\alpha_a \int_{V_a} \left|\vec{E}_s\left(\vec{R}, k_s, \gamma_s\right)\right|^2 dv \qquad (13)$$

$$\tilde{W}_{abs(s)} = Z_0^{-1}\mathrm{Im}\alpha_d \mathrm{Re}\alpha_d \int_{V_d} \left|\vec{E}_s\left(\vec{R}, k_s, \gamma_s\right)\right|^2 dv \qquad (14)$$

where we use the symbol $\sim$ to emphasize that the corresponding quantities are built on the LEP solutions and depend on γ.

Hence, for the sth mode having the wavenumber k_s, the power lost for radiation is balanced by the "negative absorption" (i.e., modal gain as the power generated in the active region), provided that the material gain equals γ_s. So, this is the "gain = loss" condition derived in a rigorous way.

However, besides of the real part, CPT expressed as (6) has also the imaginary part which leads to

$$2\mathrm{Im}\Pi_s = k_s \int_V \left[Z_0^{-1}\mathrm{Re}\left(\nu^2\right)|E_s|^2 - Z_0|\vec{H}_s|^2\right] dv \qquad (15)$$

where the domain V is arbitrary. In the limit of $S \to \infty$ as a circle of large radius, the LHP of (15) is zero because, due to (5)

$$\Pi = \frac{1}{2Z_0k^2}\int_0^{2\pi}\int_0^{\pi}\left[\left|\Phi^{(1)}\right|^2 + \left|\Phi^{(2)}\right|^2\right]\cos\theta d\theta d\varphi \qquad (16)$$

and the same is valid if $V = V_{\min}$ because of the continuity of Π. Therefore, we obtain

$$\int_{V_{\min}} \left[Z_0^{-1}\mathrm{Re}(\nu^2)|\vec{E}_s|^2 - Z_0|\vec{H}_s|^2\right] dv = 0 \qquad (17)$$

which means that the fractions of the power contained in the electric and magnetic field of any mode inside the cavity volume $V_{\min}$ equal each other. The same is valid in the whole space. Note that this property holds true for any mode in both passive and active open cavities, on resonance.

III. Uniformly Active Cavities

An open cavity can be uniformly active, i.e., $V_{\min} = V_a = V$, only if it is a slab, a circular cylinder, or a sphere. In this case, (13) is proportional to the E-field power stored in the cavity

$$\tilde{W}_{gain(s)} = \frac{2\gamma_s\alpha}{\alpha^2 - \gamma_s^2}\tilde{W}_s \qquad (18)$$

$$\tilde{W}_s = (1/2Z_0)\left(\alpha^2 - \gamma_s^2\right)\int_V \left|\vec{E}_s\left(\vec{R}, k_s, \gamma_s\right)\right|^2 dv. \qquad (19)$$

The latter quantity, if the E-field is normalized by its maximum value, is known as *active-cavity effective mode volume*. The quantity $k_s\tilde{W}_{rad(s)}$ or $k_s\tilde{W}_{gain(s)}$ can be considered as the *active-cavity effective emission cross section*, and, by analogy to the conventional passive cavities, the *active-cavity Q factor* can be defined as

$$\tilde{Q}_s = \tilde{W}_s/\tilde{W}_{rad(s)}. \qquad (20)$$

Then, the OT (12) takes the form

$$\gamma_s = \left(\alpha^2 - \gamma_s^2\right)\left(\alpha\tilde{Q}_s\right)^{-1} \qquad (21)$$

where all quantities make sense only for a specific sth mode.

A. Slab Cavity

Consider a 1-D active slab in free space, infinite along the x-axis and of width w along the y-axis (Fabry–Perot etalon). In this case, there is no difference between the two polarizations, so that, say, the E_z field component of a lasing mode is [45]

$$E_z = AU(y), \quad U(y) = \begin{cases} S^{\pm}(\kappa\nu\eta), & |\eta| < 1 \\ S^{\pm}(\kappa\nu)e^{i\kappa(|\eta|-1)}, & |\eta| > 1 \end{cases} \qquad (22)$$

where A is a constant, $\eta = y/w$, $\kappa = kw$, $S^+(.) = \cos(.)$, $S^-(.) = \sin(.)$, and (κ, γ) satisfy one of the two equations

$$e^{-i\nu\kappa} = \pm(\nu - 1)/(\nu + 1) \qquad (23)$$

with the upper (lower) sign for the symmetric (antisymmetric) modes. Solutions to (23) are discrete values (κ_n, γ_n) with $n = 0, 2, \ldots$ and $n = 1, 3, \ldots$, respectively.

Then we find that the quantities entering (20) are

$$\tilde{W}_n = A^2 w\frac{(\alpha^2 - \gamma_n^2)}{Z_0\kappa_n}\left[\frac{\sinh(\gamma_n\kappa_n)}{\gamma_n} - (-1)^n\frac{\sin(\alpha\kappa_n)}{\alpha}\right] \qquad (24)$$

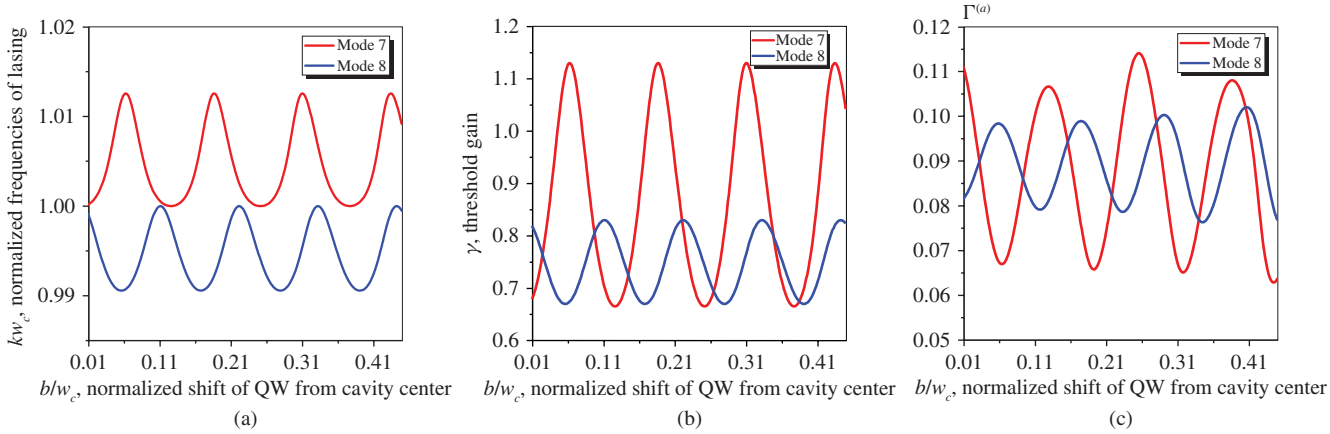

Fig. 4. Same as in Fig. 3 as a function of the normalized off-center shift of the QW occupying 1/10 of the slab cavity width. $\alpha_a = \alpha_p = 3.53$.

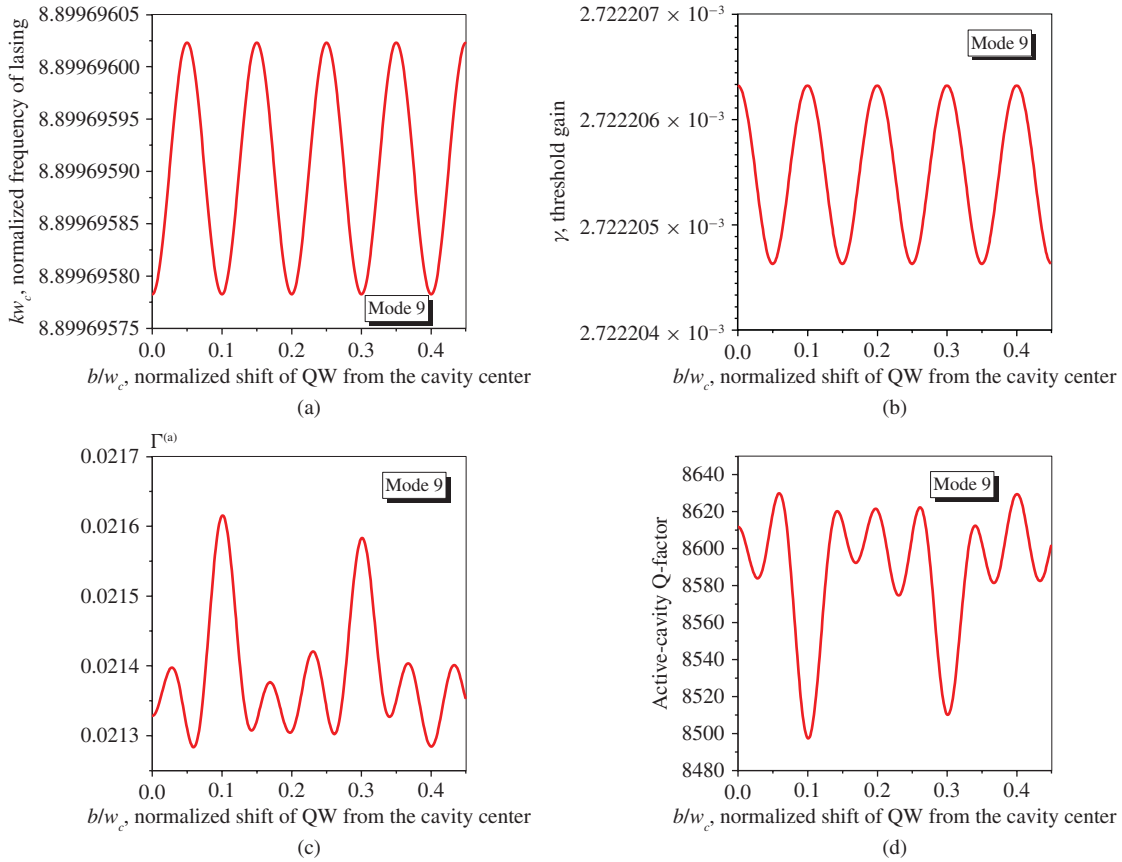

Fig. 5. (a)–(c) Same as in Fig. 4 and (d) active-cavity Q factor for a QW equipped slab cavity sandwiched between two identical DBRs of $M = 20$ pairs of layers each. $\alpha_a = \alpha_p = 3.53$.

$$\tilde{W}_{rad(n)} = A^2 w \frac{2}{Z_0 \kappa_n} \left| v_n S^{\pm}\left(\frac{v_n \kappa_n}{2}\right)\right|^2 \tag{25}$$

so that, after some algebra, the OT (21) takes the form

$$\frac{\alpha \sinh(\gamma_n \kappa_n) - (-1)^n \gamma_n \sin(\alpha \kappa_n)}{\alpha^2 + \gamma_n^2} = \cosh(\gamma_n \kappa_n) + (-1)^n \cos(\alpha \kappa_n). \tag{26}$$

Note that to make (24) the effective mode volume, the normalization constant should be taken as

$$A \equiv A_n = \max_{|y|<w}{}^{-1} |U_n(y)|, \quad U_n(y) = U(y, \kappa_n, \gamma_n). \tag{27}$$

B. Circular Cavity

Consider a 2-D active cavity of radius a in free space. In this case, the two polarization states are different. Respectively, the E_z or $Z_0 H_z$ field component of a lasing mode can be denoted as $AU(\vec{r})$ (see [40]), where

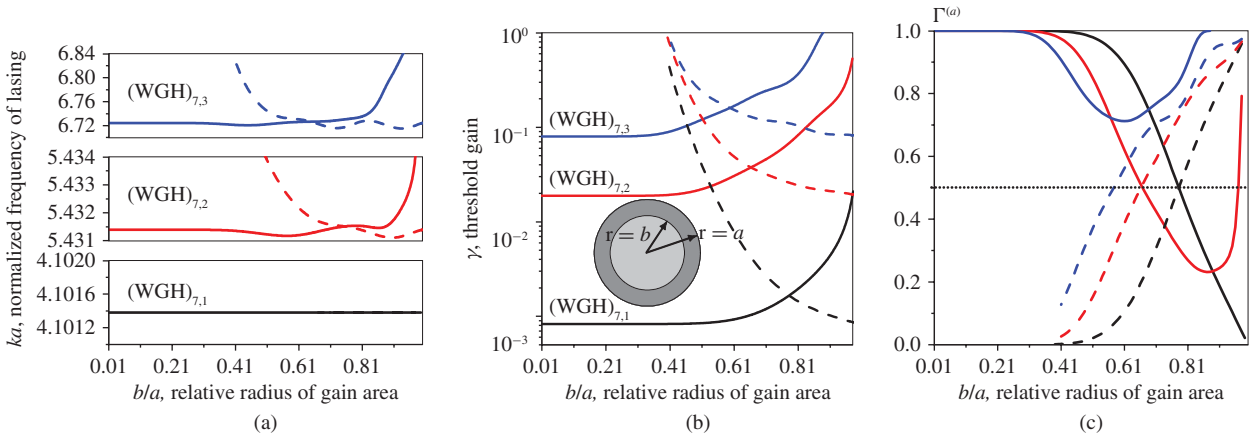

Fig. 6. (a) Normalized lasing frequencies, (b) thresholds, and (c) overlap coefficients of the $(H_z)_{7,n}$, $n = 1, 2, 3$ modes in the disk cavity vs. the normalized outer (solid curves) and inner (dashed curves) radius of the concentric ring-like or circular active region, respectively. $\alpha_a = \alpha_p = 2.63$.

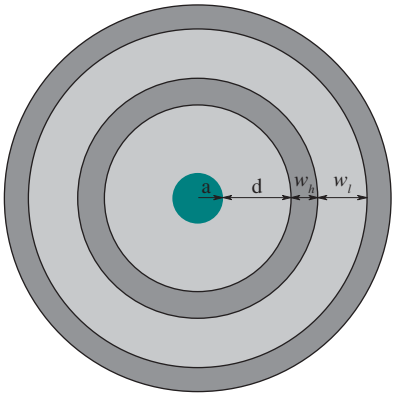

Fig. 7. 2-D geometry of an active circular disk concentrically loaded with a finite number of double passive rings forming ABR.

$$U(r,\varphi) = \left\{ \begin{array}{ll} J_m(\kappa\nu\rho), & \rho < 1 \\ \frac{J_m(\kappa\nu)}{H_m(\kappa)} H_m(\kappa\rho), & \rho > 1 \end{array} \right\} \cos m\varphi. \qquad (28)$$

Here, A is an arbitrary constant, $m = 0, 1, \ldots,$ $\rho = r/a$, $\kappa = ka$, $\nu = \alpha - i\gamma$, and $J_m(.)$ and $H_m(.) = H_m^{(1)}(.)$ are the Bessel and the first-kind Hankel functions, respectively. The values κ and γ satisfy complex-valued characteristic equations for the E_z/H_z polarised modes, derived as

$$J_m(\kappa\nu)H_m'(\kappa) - \nu^{\pm 1} J_m'(\kappa\nu)H_m(\kappa) = 0, \quad m = 0, 1, \ldots . \qquad (29)$$

These roots can be numbered as $(\kappa_{mn}, \gamma_{mn})$ with $n = 1, 2, \ldots$.

Thus, the quantities in (20) are found to be

$$\tilde{W}_{mn} = A^2 a^2 \frac{(\alpha^2 - \gamma_{mn}^2)}{2Z_0 \alpha^2 \gamma_{mn} \kappa_{mn}} \mathrm{Im}\left[\nu_{mn} \Omega_m(\nu_{mn}\kappa_{mn})\right] \qquad (30)$$

$$\tilde{W}_{rad(m,n)} = \frac{A^2 a^2}{Z_0 \kappa_{mn}^2} \left| \frac{J_m(\kappa_{mn}\nu_{mn})}{H_m(\kappa_{mn})} \right|^2 \qquad (31)$$

where

$$\Omega_m(x) = J_{m-2}(x) J_{m-1}(x^*) + J_m(x) J_{m+1}(x^*) \qquad (32)$$

and

$$A \equiv A_{m,n} = \max_{r<a}{}^{-1} \left| U_{m,n}(r,\varphi) \right|. \qquad (33)$$

Finally, the OT (21) reduces to

$$2\alpha \left| \frac{J_m(\kappa_{mn}\nu_{mn})}{H_m(\kappa_{mn})} \right|^2 = \pi \kappa_{mn} \mathrm{Im}\left[\nu_{mn} \Omega_m(\kappa_{mn}\nu_{mn})\right]. \qquad (34)$$

As computations show, on finding the eigenpair (κ_s, γ_s) from characteristic equations (23) or (29), i.e., on resonance, identities (26) and (34) are satisfied with machine precision.

Effective mode volume plays very important role in the cavity quantum electrodynamics (QED) [27]. However, in QED this quantity appears from heuristic considerations. Besides, one and the same definition is used for active and passive cavities; the integration is usually taken only over V_d but sometimes is extended to a part of the space outside the dielectrics and even outside of $V_{\min}$ (as, for instance, in [26, p. 218] and in [53]). In contrast, here we have introduced $\tilde{W}_s$ in a rigorous and unambiguous way based only on mathematical manipulations with Maxwell equations, i.e., from first principles.

IV. Partially Active Cavities and Overlap Coefficients

The laser configurations where the active region does not coincide with the whole cavity (i.e., $V_p \neq 0$ in Fig. 1) are the most interesting, because they are intractable within the passive-cavity analysis. Such a situation is met if one uses a sharply focused pump beam in optically pumped laser. Besides, combination of separated active and passive regions is typical for the cavities with DBRs and for photonic-molecule lasers using selective pumping. Moreover, this is common for all injection lasers, which are known to be extremely vulnerable to the placement of electrodes. This is because the concentration of carriers is obviously greater in the immediate vicinity of the electrode than far from it.

The OT for lasers sheds important light on the behavior of modal thresholds in the cavities with partial active regions. Indeed, for each sth mode one can introduce the quantity

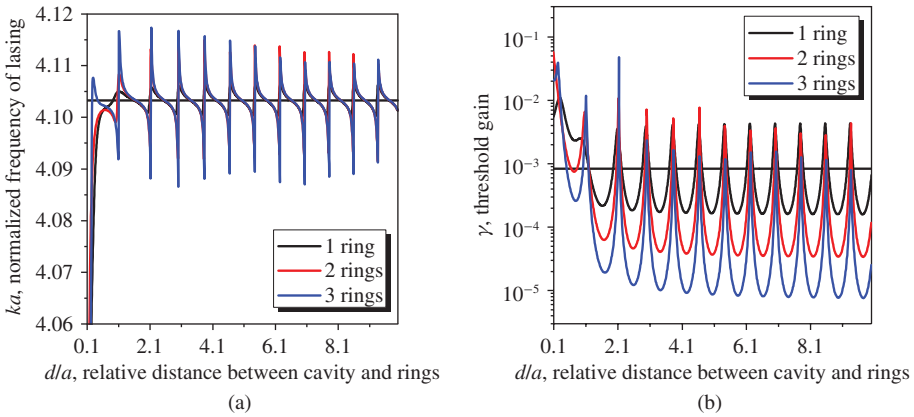

Fig. 8. (a) Normalized lasing frequencies and (b) thresholds of the $(H_z)_{7,1,p,1}$ supermode in the disk loaded with passive ABR vs. the normalized air gap between the disk and the first ring. $w_h/w_l = 1$, $w_h = 0.2a$, $\alpha_a = \alpha_h = 2.63$, $\alpha_l = 1$.

$\Gamma_s^{(a)} \le 1$ as follows:

$$\Gamma_s^{(a)} = \tilde{W}_s^{(a)}/\tilde{W}_s$$
$$\tilde{W}_s^{(a)}(k_s,\gamma_s) = (1/2Z_0)\left(\alpha_a^2 - \gamma_s^2\right)\int_{V_a}\left|\vec{E}_s\left(\vec{R},k_s,\gamma_s\right)\right|^2 dv$$
$$\tilde{W}_s(k_s,\gamma_s) = (1/2Z_0)\int_{V_{\min}} Re(\nu^2)\left|\vec{E}_s\left(\vec{R},k_s,\gamma_s\right)\right|^2 dv \quad (35)$$

where $\nu = \alpha_d$ in V_d and 1 in V_f, and $V_{\min} = V_a + V_d + V_f$.

From this definition, it is clear that $\Gamma_s^{(a)}$ is the fraction of E-field power contained in the active region. It is also the *overlap coefficient* between the active region and the modal E-field (a.k.a. *mode confinement factor* [26], [27]). This is a strictly discrete quantity having values linked to specific modes.

This enables us to rewrite the OT (12) in the following manner

$$\gamma_s = \frac{\alpha_a}{\Gamma_s^{(a)}(k_s,\gamma_s)}\ \frac{1}{\tilde{Q}_s(k_s,\gamma_s)} \quad (36)$$

where now $\tilde{Q}_s = \tilde{W}_s/[\tilde{W}_{rad(s)} + \tilde{W}_{abs(s)}]$. Further investigation of (36) assuming that the threshold is small, $\gamma_s \ll 1$, shows that the first-order approximation to γ_s is obtained if one takes the mode field components and the frequency as for a passive cavity ($\gamma_s = 0$)

$$\gamma_s = \frac{\alpha_s}{\Gamma_s^{(a)}(k_s,0)Q_s} + O(\gamma_s^2). \quad (37)$$

Equation (37) tells that, in order to achieve low threshold in the active (pump on) cavity, it is not enough to have a high Q factor of the same mode in the passive (pump off) cavity. The overlap of the mode E-field with the active region is equally important and can dramatically spoil the result: this happens, for instance, with the quasi-WG modes in a stadium-cavity laser if the electrode is placed at its center [22], [23].

Note that in QED it is considered (for instance, see [27 pp. 287, 291, 300]) that the smaller the effective mode volume, the lower the threshold of lasing. Our formulas (20) and (36) convincingly show that from the viewpoint of Maxwell equations this is not true. In fact, the role of the effective mode volume is just the opposite, as $\tilde{W}_s$ enters the denominator of the RHP of (36); however, this role is balanced by the mode losses (including emission loss, $\tilde{W}_{rad(s)}$) in the numerator, as these two quantities "breath" together. The real figure of merit of the mode in active cavity is its Q factor $\tilde{Q}_s$, which can be approximated by the passive-cavity counterpart Q_s.

Similar to $\Gamma_s^{(a)}$, another quantity can be introduced to characterize the overlap of the passive part of the cavity, within the minimum sphere, with modal E-field

$$\Gamma_s^{(p)} = \tilde{W}_s^{(p)}/W_s, \quad \tilde{W}_s^{(p)} = (1/2Z_0)\int_{V_p} \mathrm{Re}\left(\alpha_p^2\right)\left|\vec{E}_s\right|^2 dv \quad (38)$$

so that $\Gamma_s^{(a)} + \Gamma_s^{(p)} = 1$. Note that $\Gamma_s^{(p)}$ may itself be a sum of the partial coefficients and may contain a free-space term.

V. VCSEL-Like 1-D Configurations

In this section, we briefly consider the results of the LEP study for the 1-D plane-layered media containing active layers. In fact, this demonstrates that the whole semiclassical laser physics is conveniently embedded into the LEP formalism. This is because rays and waves are equivalent in the 1-D case.

A. QW Inside a Passive Fabry–Perot Etalon

Consider a passive dielectric slab (a.k.a. Fabry–Perot etalon, Fig. 2) with refractive index α and thickness w_c containing a quantum well (QW) of the index $\nu = \alpha - i\gamma$ and thickness w_a.

The results computed for the modes $n = 7, 8$ in a resonator with a centrally placed QW of varying width are presented in Fig. 3. As expected from elementary considerations, if the QW shrinks to zero, the mode frequencies remain stable while the thresholds grow infinitely as $\gamma_n = O(w_c/w_a)$. The active-region overlap coefficients [Fig. 3(c)] display remarkable agreement with inverse values of the relevant threshold curves.

Fig. 4 demonstrates, for the same modes, the effect of the QW shift from the center of the slab cavity; the QW width is 1/10 of the whole cavity. One can see that both the threshold and the overlap dependences display a series of periodically spaced minima and maxima. The maxima of the overlap coefficients correspond to the good matching of the QW with the modal E-field antinodes; this leads to the threshold minima as predicted by (36). Note that modes $n = 1$ and 2 have very high values of threshold gain [45], which makes them both impractical and more difficult for numerical analysis.

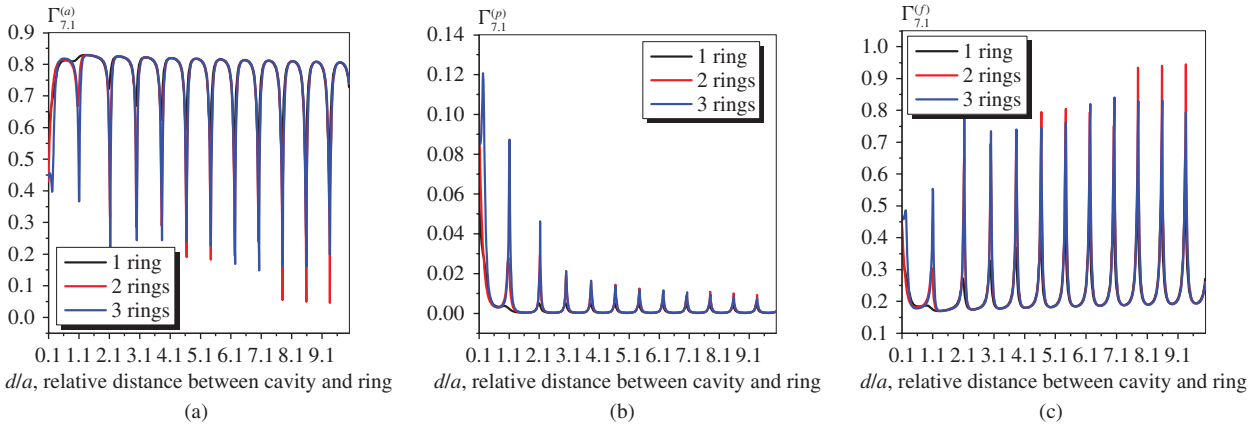

Fig. 9. (a) Active-region, (b) passive-ring, and (c) free-space (airgap) overlap coefficients for the same disk-in-ABR geometry variation as in Fig. 8.

B. QW-Equipped Cavity Between Two DBRs

If a slab-like cavity with an embedded QW is sandwiched between two DBRs opening into free space, then the thresholds of those modes whose frequencies get into the stop-band of DBRs obtain lower values [31]–[33]. This effect is in the core of the VCSEL design.

The LEP characteristic equation is built using the transfer matrix method (TMM) [31]–[33], [45] and conditions (2)–(4).

In Fig. 5 we present the dependences of the lasing frequency, threshold, QW overlap coefficient, and active cavity Q factor of the lasing mode $n = 9$ on the relative shift of a narrow QW from the central position in a cavity placed between two identical 20-pair DBRs. Note that, in such a cavity, the threshold of lasing for the mode whose frequency is in the DBR stopband is determined by the number of DBR layer pairs [45].

Unlike a simple Fabry–Perot etalon, this configuration has multiple passive "subcavities" optically coupled to the "main cavity" with active region.

As a result, here the mode Q factor [see (36)] depends on the QW shift in stronger manner than for a simple slab cavity in free space. Therefore, the correlation between the threshold and the QW overlap coefficient is less impressive although the locations of minima and maxima again coincide. Still, some threshold maxima are higher than the others, which is explained by the effect of the E-field pulling into the DBR layers [46], besides that of the QW mismatch with the modal field inside the internal cavity.

VI. Active Disks Loaded with Passive Rings

In this section, we consider the LEP solutions for several 2-D circular-concentric laser configurations.

A. Active Disk with a Passive Rim or Central Circle

As a simplest example, consider the modes in a thin disk with a radially piecewise active region ($\alpha_a = \alpha_d = \alpha$) (see also [41]). In this geometry, modes with different azimuth indices m satisfy independent characteristic equations, built by using TMM [6]–[8] and conditions (2)–(4). In a uniformly active disk, the WG modes correspond to the condition $m/\alpha <$ $k_{mn}a < m$, and their thresholds behave asymptotically as $\gamma_{mn} = O(e^{-\alpha k_{mn}a}) \ll 1$ while $k_{mn}a = O(m+n)$.

The plots in Fig. 6(a) and (b) demonstrate the dynamics of the modal frequencies and thresholds for the WG modes $(\mathrm{H}_z)_{7,n}$ $(n = 1, 2, 3)$ in a circular cavity with active region being either a centered circle of varying radius b or a ring of varying inner radius b. As visible, if b varies, the threshold curves corresponding to the inner circular active region and outer ring-like one cross each other (see also Fig. 9 of [41]). What is remarkable is that, at the crossing points, each mode's threshold is exactly twice as in the uniformly active disk (by 0.3 in logarithmic scale). Keeping in mind that the contrast between the active and passive parts of the considered cavity is very small (it has the order of γ), and the WG-mode frequency and field pattern vary as $O(\gamma)$, we may conclude that (36) tells that this effect can be explained by a drop in the modal gain overlap factors to $\Gamma^{(a)}_{7,n} = 1/2$. The plots in Fig. 6(c) provide evidence to this suggestion.

Moreover, if one pumps any isolated spot and leaves the remaining ring-like domain passive, and vice versa, the analogous curves, for each mode, will also cross at the point of twice higher threshold than for the uniformly active disk. This is because in either case we split the cavity into two parts, passive and active. This observation is a verification of obtained numerical results and a proof of OTs practicality.

B. Active Disk Embedded into ABR

A more complicated laser configuration which can be approximately reduced to the 2-D formulation and involves only concentric circular boundaries is depicted in Fig. 7. This is an active disk at the center of M-pair ABR; such lasers have been studied in the 2000s [6]–[8], [54]–[57]. Here, the underlining idea is to use a relatively small active disk and still obtain ultralow threshold of lasing due to the optical confinement provided by ABR.

Usually in the experiments only the central disk is pumped, i.e., is active, while the ABR area remains passive to avoid multimode lasing [54]–[57]. Although this geometry is actually a rotationally symmetric 3-D one [57], [38], [39], still an advanced 2-D analysis of ABR-loaded active circular cavity using the LEP approach is interesting as a tool for optimization

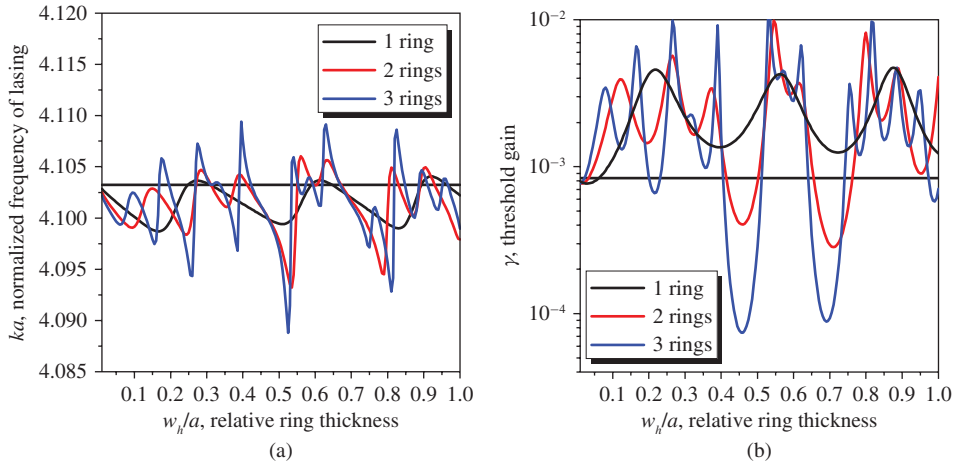

Fig. 10. (a) Normalized lasing frequencies and (b) thresholds of the $(H_z)_{7,1,p,q}$ supermodes in the disk-in-ABR laser vs. the normalized ring thickness $d = 0.5a$, $w_h/w_l = 1$, $\alpha_a = \alpha_h = 2.63$, $\alpha_l = 1$.

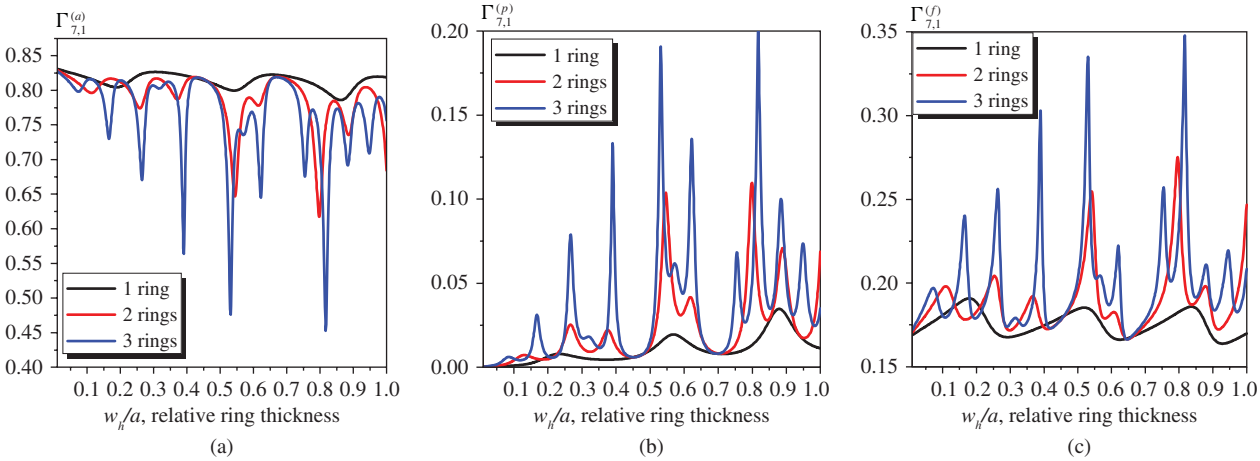

Fig. 11. (a) Active-region, (b) passive-ring and (c) free-space (air gap) overlap coefficients for the same disk-in-ABR geometry variation as in Fig. 10.

of the in-plane confinement in such lasers. Using TMM for each value of the azimuth index m, we reduce the problem to a set of independent determinantal equations (see [6], [7], [46]), whose orders equal to the number of circular boundaries, i.e., $2M + 1$. The results of computations are demonstrated in Figs. 8–11 for the supermode $(\mathrm{H}_z)_{7,1,p,q}$ in active disks loaded with 1, 2, and 3 passive rings.

In Figs. 8 and 9, the lasing frequencies and thresholds, and overlap coefficients, respectively, are shown for varying separation between the active disk and the first ring d/a, fixed duty cycle $\delta = w_h/w_l$, and ring thickness, w_h.

Note that in this configuration multiple concentric partial domains are present. As a result, it is not enough to use one radial index to characterize a mode; in fact, $2M + 1$ radial indices are needed to show the number of additional field variations in the air gaps and rings. If the gap and ring widths are identical, we may use three radial indices (n, p, q). Such a complicated behavior points to the hybrid nature of "supermodes" in the disk optically coupled with ABR [46].

In Figs. 10 and 11, we show the same quantities as a function of the ring thickness for the fixed values of the other parameters.

It is apparent that the number of ring pairs can be kept small if the contrast between the higher and lower ABR refraction indices α_h and α_l is large. Here, we took $\alpha_a = \alpha_h = 2.63$ and $\alpha_f = \alpha_l = 1$ (air), and one can see that, in the ABR stopband, adding a pair of concentric layers reduces the threshold of the $(\mathrm{H}_z)_{7,1,p,q}$ supermode nearly by an order of magnitude. Plots of the partial domain overlap coefficients (see Figs. 9–11) support the prediction that the threshold jumps up each time the E-field is pushed from the active region because of strong coupling to the modes of the rings of ABR. Note that here the field of the mode can be pulled into both dielectric and air rings and the relevant overlap coefficients reach high values. This is because the ring thickness becomes comparable to the wavelength in the ring material.

VII. Conclusion

We have highlighted important points of the Maxwell eigenvalue analysis for a dielectric microcavity modified for the presence of active regions, i.e., the LEP. This formulation can be called a "warm-cavity" electromagnetic model of laser to emphasize its position between the cold-cavity (passive and linear) and hot-cavity (active and nonlinear) models.

We have also presented the OT for the lasers considered in linear formulation. The derived expressions can be used for verification of numerical results obtained for particular configurations. Moreover, they have enabled us to propose, for the first time, rigorous mathematical definitions of the open-resonator volume (as a minimum sphere), the effective mode volume, and the mode-active-region overlap coefficient: this, in fact, provides grounding to these quantities used in semi-classical laser physics and QED as phenomenological ones.

We have shown several numerical examples demonstrating the nontrivial interplay between passive and active parts of the laser cavities in their competition for the mode field, even in the separable 1-D and 2-D configurations.

This approach goes far beyond traditional passive-cavity simulations and opens the new and exciting area of advanced linear modeling of microcavity lasers. The tailoring of the active region shape can be an efficient tool for the threshold control and manipulation while keeping the emission frequency essentially untouched. The latter is true so far as the gain-induced contrast in the cavity is small, which is valid for the low-threshold modes such as WG-like or DBR-assisted ones. In fact, the LEP approach gives a firm mathematical footing to the phenomenological semiclassical laser theory and holds true for arbitrary laser configurations where Fabry–Perot-like or, more generally, ray-tracing descriptions are not applicable.

REFERENCES

[1] A. Yariv, *Quantum Electronics*. New York: Wiley, 1989.

[2] D. J. Piprek, *Optoelectronic Devices: Advanced Simulation and Analysis*. Berlin, Germany: Springer-Verlag, 2005.

[3] M. Streiff, A. Witzig, M. Pfeiffer, P. Royo, and W. Fichtner, "A comprehensive VCSEL device simulator," *IEEE J. Sel. Topics Quantum Electron.*, vol. 9, no. 3, pp. 879–891, May–Jun. 2003.

[4] T. M. Benson, S. V. Boriskina, P. Sewell, A. Vukovic, S. C. Greedy, and A. I. Nosich, "Micro-optical resonators for microlasers and integrated optoelectronics," in *Frontiers of Planar Lightwave Circuit Technology: Design, Simulation and Fabrication*, S. Janz, J. Ctyroky, and S. Tanev, Eds. Berlin, Germany: Springer-Verlag, 2005, pp. 40–70.

[5] N. C. Frateschi and A. F. Levi, "The spectrum of microdisk lasers," *J. Appl. Phys.*, vol. 80, no. 2, pp. 644–653, 1996.

[6] M. A. Kaliteevski, R. A. Abram, and V. V. Nikolaev, "Optical eigenmodes of a cylindrical microcavity," *J. Mod. Opt.*, vol. 47, no. 4, pp. 677–684, 2000.

[7] J. Scheuer and A. Yariv, "Annular Bragg defect mode resonators," *J. Opt. Soc. Am. B*, vol. 20, no. 11, pp. 2285–2291, 2003.

[8] A. Jebali, D. Erni, S. Gulde, R. F. Mahrt, and W. Bachtold, "Analytical calculation of the Q-factor for circular-grating microcavities," *J. Opt. Soc. Am. B*, vol. 24, no. 4, pp. 906–915, 2007.

[9] J. U. Noeckel and A. D. Stone, "Chaotic light: A theory of asymmetric resonant cavities," in *Optical Processes in Microcavities*, R. K. Chang and A. J. Campillo, Eds. Singapore: World Scientific, 1996, pp. 389–426.

[10] J. U. Noeckel and R. K. Chang, "2-D microcavities: Theory and experiments," in *Cavity-Enhanced Spectroscopies*, R. D. van Zee and J. P. Looney, Eds. San Diego, CA: Academic, 2002.

[11] H. G. L. Schwefel, H. E. Tureci, A. D. Stone, and R. K. Chang, "Progress in asymmetric resonant cavities: Using shape as a design parameter in dielectric microcavity lasers," in *Optical Microcavities*, K. Vahala, Ed. Singapore: World Scientific, 2004, pp. 415–496.

[12] Y. Z. Huang, W. H. Guo, and L. J. Yu, "Analysis of mode characteristics for equilateral triangle semiconductor microlasers with imperfect boundaries," *Proc. IEE Optoelectron.*, vol. 151, no. 4, pp. 202–204, Aug. 2004.

[13] A. V. Boriskin, S. V. Boriskina, A. Rolland, R. Sauleau, and A. I. Nosich, "Test of the FDTD accuracy in the analysis of the scattering resonances associated with high-Q whispering-gallery modes of a circular cylinder," *J. Opt. Soc. Am. A*, vol. 25, no. 5, pp. 1169–1173, 2008.

[14] S.-L. Qiu and Y.-P. Li, "Q-factor instability and its explanation in the staircased FDTD simulation of high-Q circular cavity," *J. Opt. Soc. Am. A*, vol. 26, no. 9, pp. 1664–1674, 2009.

[15] J. Niegemann, W. Pernice, and K. Busch, "Simulation of optical resonators using DGTD and FDTD," *J. Pure Appl. Opt. A*, vol. 11, no. 11, pp. 4015–4025, 2009.

[16] A. I. Nosich, E. I. Smotrova, S. V. Boriskina, T. Benson, and P. Sewell, "Trends in microdisk laser research and linear optical modeling," *Opt. Quantum Electron.*, vol. 39, no. 15, pp. 1993–1995, 2007.

[17] J. Wiersig, "Hexagonal dielectric resonators and microcrystal lasers," *Phys. Rev. A*, vol. 67, no. 2, pp. 023807-1–023807-12, Feb. 2003.

[18] S.-Y. Lee, M. S. Kurdoglyan, S. Rim, and C.-M. Kim, "Resonance patterns in a stadium-shaped microcavity," *Phys. Rev. A*, vol. 70, no. 2, p. 023809, 2004.

[19] S. V. Boriskina, P. Sewell, T. M. Benson, and A. I. Nosich, "Accurate simulation of 2-D optical microcavities with uniquely solvable boundary integral equations and trigonometric Galerkin discretization," *J. Opt. Soc. Am. A*, vol. 21, no. 3, pp. 393–402, 2004.

[20] J. Wiersig, "Formation of long-lived, scarlike modes near avoided resonance crossings in optical microcavities," *Phys. Rev. Lett.*, vol. 97, p. 253901, Sep. 2006.

[21] R. Dubertrand, E. Bogomolny, N. Djellali, M. Lebental, and C. Schmit, "Circular dielectric cavity and its deformations," *Phys. Rev. A*, vol. 77, no. 1, pp. 013804–013820, 2008.

[22] C. Gmachl, F. Cappasso, E. E. Narimanov, J. U. Noeckel, A. D. Stone, J. Faist, and D. L. Sivco, "High-power directional emission from microlasers with chaotic resonances," *Science*, vol. 280, pp. 1556–1564, Jun. 1998.

[23] H. E. Tureci and A. D. Stone, "Mode competition and output power in regular and chaotic dielectric cavity lasers," in *Proc. SPIE*, vol. 5708. 2005, pp. 255–270.

[24] T. Harayama, P. Davis, and K. S. Ikeda, "Nonlinear whispering gallery modes," *Phys. Rev. Lett.*, vol. 82, no. 19, pp. 3803–3808, 1999.

[25] N. B. Rex, R. K. Chang, and L. J. Guido, "Threshold lowering in GaN micropillar lasers by means of spatially selective optical pumping," *IEEE Photon. Technol. Lett.*, vol. 13, no. 1, pp. 1–3, Jan. 2001.

[26] M. M. Mazumder, D. Q. Chowdhury, S. C. Hill, and R. K. Chang, "Optical resonances of a spherical dielectric microcavity," in *Optical Processes in Microcavities*, R. K. Chang and A. J. Campillo, Eds. Singapore: World Scientific, 1996, pp. 209–256.

[27] H. Yokoyama and K. Ujihara, *Spontaneous Emission and Laser Oscillation in Microcavities*. Boca Raton, FL: CRC, 1995.

[28] M. Kerker, "Resonances in electromagnetic scattering by objects with negative absorption," *Appl. Opt.*, vol. 18, no 8, pp. 1180–1189, 1979.

[29] N. G. Alexopoulos and N. K. Uzunoglu, "Electromagnetic scattering from active objects: Invisible scatterers," *Appl. Opt.*, vol. 17, no. 2, pp. 235–239, 1978.

[30] A. G. Vlasov and O. O. Skliarov, "Electromagnetic boundary value problem for a radiating dielectric cylinder with reflectors at both ends," *Radio Eng. Electron. Phys.*, vol. 22, no. 1, pp. 17–23, 1977.

[31] S. W. Corzine, R. S. Geels, J. W. Scott, R.-H. Yan, and L. A. Coldren, "Design of Fabry-Perot surface-emitting lasers with a periodic gain structure," *IEEE J. Quantum Electron.*, vol. 25, no. 6, pp. 1513–1524, Jun. 1989.

[32] B. Klein, L. F. Register, K. Hess, D. G. Deppe, and Q. Deng, "Self-consistent Green's function approach to the analysis of dielectrically apertured VCSELs," *Appl. Phys. Lett.*, vol. 73, no. 23, pp. 3324–3326, 1998.

[33] M. J. Noble, J. P. Loehr, and J. A. Lott, "Analysis of microcavity VCSEL lasing modes using a full-vector weighted index method," *IEEE J. Quantum Electron.*, vol. 34, no. 10, pp. 1890–1903, Oct. 1998.

[34] J. V. Campenhout, P. Bienstman, and R. Baets, "Band-edge lasing in gold-clad photonic-crystal membranes," *IEEE J. Sel. Areas Commun.*, vol. 23, no. 7, pp. 1418–1423, Jul. 2005.

[35] A. Mizrahi, V. Lomakin, B. A. Slutsky, M. P. Nezhad, L. Feng, and Y. Fainman, "Low threshold gain metal coated laser nanoresonators," *Opt. Lett.*, vol. 33, no. 11, pp. 1261–1263, 2008.

[36] C. Manolatou and F. Rana, "Subwavelength nanopatch cavities for semiconductor plasmon lasers," *IEEE J. Quantum Electron.*, vol. 44, no. 5, pp. 435–447, May 2008.

[37] X. Sun, J. Scheuer, and A. Yariv, "Optimal design and reduced threshold in vertically emitting circular Bragg disk resonator lasers," *IEEE J. Sel. Topics Quantum Electron.*, vol. 13, no. 2, pp. 359–366, Mar.–Apr. 2007.

[38] J. Scheuer, "Radial Bragg lasers: Optimal design for minimal threshold levels and enhanced mode discrimination," *J. Opt. Soc. Am. B*, vol. 24, no. 9, pp. 2178–2184, 2007.

[39] X. Sun and A. Yariv, "Surface-emitting circular DFB, disk, and ring-Bragg resonator lasers with chirped gratings, part II," *Opt. Exp.*, vol. 17, no. 1, pp. 1–6, 2009.

[40] E. I. Smotrova and A. I. Nosich, "Mathematical study of the 2-D lasing problem for the whispering-gallery modes in a circular dielectric microcavity," *Opt. Quantum Electron.*, vol. 36, nos. 1–3, pp. 213–221, 2004.
[41] E. I. Smotrova, A. I. Nosich, T. M. Benson, and P. Sewell, "Cold-cavity thresholds of microdisks with uniform and non-uniform gain: Quasi-3-D modelling with accurate 2-D analysis," *IEEE J. Sel. Topics Quantum Electron.*, vol. 11, no. 5, pp. 1135–1142, Sep.–Oct. 2005.
[42] E. I. Smotrova, A. I. Nosich, T. M. Benson, and P. Sewell, "Optical coupling of the whispering gallery modes of two identical microdisks and its effect on photonic molecule lasing," *IEEE J. Sel. Topics Quantum Electron.*, vol. 12, no. 1, pp. 78–85, Jan.–Feb. 2006.
[43] E. I. Smotrova, A. I. Nosich, T. M. Benson, and P. Sewell, "Threshold reduction in a cyclic photonic molecule laser composed of identical microdisks with whispering-gallery modes," *Opt. Lett.*, vol. 31, no. 7, pp. 921–923, 2006.
[44] E. I. Smotrova, A. I. Nosich, T. Benson, and P. Sewell, "Ultralow lasing thresholds of the π-type supermodes in cyclic photonic molecules composed of sub-micron disks with monopole and dipole modes," *IEEE Photon. Technol. Lett.*, vol. 18, no. 19, pp. 1993–1995, Oct. 2006.
[45] V. O. Byelobrov and A. I. Nosich, "Mathematical analysis of the lasing eigenvalue problem for the optical modes in a layered dielectric cavity with a quantum well and distributed Bragg reflectors," *Opt. Quantum Electron.*, vol. 39, nos. 10–11, pp. 927–937, 2007.
[46] E. I. Smotrova, J. Ctyroky, T. Benson, P. Sewell, and A. I. Nosich, "Lasing frequencies and thresholds of the dipole-type supermodes in an active microdisk concentrically coupled with a passive microring," *J. Opt. Soc. Am. A*, vol. 25, no. 11, pp. 2884–2892, 2008.
[47] E. I. Smotrova, J. Ctyroky, T. Benson, P. Sewell, and A. I. Nosich, "Optical fields of the lowest modes in a uniformly active thin sub-wavelength spiral microcavity," *Opt. Lett.*, vol. 34, no. 24, pp. 3773–3775, 2009.
[48] D. Colton and R. Kress, *Integral Equation Method in Scattering Theory*. New York: Wiley, 1983.
[49] A. I. Nosich, "Method of analytical regularization in the wave-scattering and eingenvalue problems: Foundations and review of solutions," *IEEE Antennas Propag. Mag.*, vol. 41, no. 3, pp. 34–49, Jun. 1999.
[50] C. Muller, *Foundations of the Mathematical Theory of Electromagnetic Waves*. Berlin, Germany: Springer-Verlag, 1969.
[51] S. Steinberg, "Meromorphic families of compact operators," *Arch. Ration. Mech. Anal.*, vol. 31, no. 5, pp. 372–379, 1968.
[52] N. Morita, N. Kumagai, and J. R. Mautz, *Integral Equation Methods for Electromagnetics*. Boston, MA: Artech House, 1990.
[53] S. M. Spillane, T. J. Kippenberg, and K. J. Vahala, "Ultrahigh-Q toroidal microresonators for cavity quantum electrodynamics," *Phys. Rev. A*, vol. 71, no. 1, pp. 1–10, 2005.
[54] A. Jebali, R. F. Mahrt, N. Moll, C. Bauer, G. L. Bona, and W. Bachtold, "Lasing in organic circular grating structures," *J. Appl. Phys.*, vol. 96, no. 6, pp. 3043–3049, 2004.
[55] J. Scheuer, W. M. J. Green, G. A. DeRose, and A. Yariv, "Low-threshold 2-D annular Bragg lasers," *Opt. Lett.*, vol. 29, no. 22, pp. 2241–2243, 2004.
[56] J. Scheuer, W. M. J. Green, G. A. DeRose, and A. Yariv, "Lasing from a circular Bragg nanocavity with an ultrasmall modal volume," *Appl. Phys. Lett.*, vol. 86, no. 25, pp. 251101-1–251101-3, 2005.
[57] J. Scheuer, W. M. J. Green, G. A. DeRose, and A. Yariv, "InGaAsP annular Bragg lasers: Theory, applications, and modal properties," *IEEE J. Sel. Topics Quantum Electron.*, vol. 11, no. 2, pp. 476–484, Mar.–Apr. 2005.

Elena I. Smotrova (S'03–M'10) was born in Kharkiv, Ukraine. She received the M.Sc. degree in applied mathematics from the Kharkiv National University, Kharkiv, in 2002, and the Ph.D. degree in radiophysics from the Institute of Radiophysics and Electronics (IRE), National Academy of Sciences of Ukraine (NASU), Kharkiv, in 2010.

She is currently a Scientist at IRE NASU. Her current research interests include integral equations, eigenvalue problems, and microcavity laser modeling.

Dr. Smotrova was the recipient of the IEEE Electron Devices Society Graduate Fellowship in 2005, and the IEEE Women in Engineering Region 8 C. Saduwa Award in 2009.

Volodymyr O. Byelobrov (S'07) was born in Kharkiv, Ukraine, in 1983. He received the M.Sc. degree in applied mathematics from the Kharkiv National University, Kharkiv, in 2006.

He is currently a Research Engineer at the Institute of Radiophysics and Electronics, National Academy of Sciences of Ukraine, Kharkiv. His current research interests include numerical methods, wave scattering by gratings, and microcavity laser modeling.

Mr. Byelobrov was the recipient of the IEEE Antennas and Propagation Society Graduate Fellowship in 2007.

Trevor M. Benson (M'95–SM'01) was born in Sheffield, U.K., in 1958. He received the Ph.D. degree in electronic and electrical engineering from the University of Sheffield, Sheffield, in 1982, and the D.Sc. degree from the University of Nottingham, Nottingham, U.K., in 2005.

He joined the University of Nottingham in 1989, where he has been a Professor at the George Green Institute for Electromagnetics Research since 1996. His current research interests include experimental and numerical electromagnetics, with emphasis on optical waveguides, lasers, glass-based photonic circuits, and electromagnetic compatibility.

Dr. Benson was a recipient of the Electronics Letters and J. J. Thomson Premiums from the Institution of Electrical Engineers (IEE), U.K., in 1994 and 1996, respectively. He is a Fellow of the IEE and the Institute of Physics, U.K.

Jiří Čtyroký (M'90–SM'99) obtained the Ph.D. degree in applied physics from the Czech Technical University (CTU), Prague, Czech Republic, in 1972, and the D.Sc. degree in electrical engineering from the Czechoslovak Academy of Sciences (CAS), Prague, in 1990.

He has been with the Institute of Radio Engineering and Electronics, CAS (now the Institute of Photonics and Electronics, Academy of Sciences of the Czech Republic, v.v.i.) since 1974, and is now Deputy Director. Since 1993, he has also been lecturing at the CTU, where he has been a Professor since 2005. His current research interests include integrated optics and guided-wave photonics including electrooptic, acoustooptic, and nonlinear interactions.

Dr. Čtyroký is a Fellow of the Institute of Physics, U.K.

Ronan Sauleau (M'04–SM'06) was born in Rennes, France, in 1972. He received the Ph.D. degree in signal processing and telecommunications from the University of Rennes 1, Rennes, in 1999.

He has been with the University of Rennes 1 since 1999, where he was elected Professor at the Institute d'Electronique et Telecommunications de Rennes in 2008. His current research interests include electromagnetics, antennas, focusing devices, and periodic structures.

Dr. Sauleau won the Young Researcher Prize in Brittany, France, in 2001, and was elected a Junior Member of the Institute Universitare de France in 2007.

Alexander I. Nosich (M'94–SM'95–F'04) was born in Kharkiv, Ukraine, in 1953. He received the Ph.D. and D.Sc. degrees in radiophysics from the Kharkiv National University, Kharkiv, in 1979 and 1990, respectively.

He has been with the Institute of Radiophysics and Electronics, National Academy of Sciences of Ukraine, Kharkiv, since 1978, where he is now a Principal Scientist. He is also with the Universite Europeenne de Bretagne, Institute d'Electronique et Telecommunications de Rennes, Universite de Rennes 1, Rennes, France. Since 1992, he has held research fellowships and visiting professorships in the EU, Turkey, Japan, and Singapore. His current research interests include methods of analytical regularization in computational electromagnetics, free-space and open-waveguide scattering, and modeling of microcavity lasers and antennas.